
Histological, Histochemical and Immunohistochemical Studies on the Prostate Gland of Bilateral Castrated Dogs

Farouk, Sameh M.¹, Amal A. M. Ahmed¹, Hashem, Mohamed A.², and *Safa H. Badran³

¹*Department of Cytology & Histology, Faculty of Veterinary Medicine, Suez Canal University, Ismailia, Egypt.*

²*Department of Surgery, Anesthesiology and Radiology, Faculty of Veterinary Medicine, Suez Canal University, Ismailia, Egypt.*

³*Department of Cytology & Histology, Faculty of Veterinary Medicine, Arish University, North Sinai, Egypt.*

* Corresponding author: **Safa H. Badran** (safabadran17@gmail.com)

Abstract

The prostate gland, an androgen-dependent organ, plays a pivotal role in male fertility. Bilateral castration, employed for therapeutic and preventive purposes in both humans and animals, prompted our investigation into the histological architecture of the prostate gland post-orchietomy in adult male dogs. Six apparently healthy male mongrel dogs (18–20 kg, 12–24 months) were divided into Control and bilateral castrated groups. A blood testosterone test was conducted, and prostatic tissues were harvested on day 20 for basic histological, histochemical, and immunohistochemical studies. Results revealed a rapid decline in serum testosterone levels, concomitant with significant histological alterations in the prostate gland. Notably, there was a substantial reduction in epithelial height and a noticeable decrease in the immunostaining affinity of androgen receptors. Additionally, a marked interstitial thickening, characterized by a significant increase in the percentage of collagen fibers, was observed. In conclusion, bilateral castration induces changes in prostatic histological architecture alongside a depletion of blood testosterone levels. These findings contribute to our understanding of the impact of castration on male reproductive organs, potentially informing therapeutic and preventive strategies for androgen-dependent conditions.

Key Words: Canine, Castration, Prostate gland, Testosterone, Androgen receptors

Introduction

The significance of male accessory genital glands in fertility is undeniable, with notable variations in types and numbers observed across mammalian species (*König & Liebich, 2020*). In dogs, the prostate gland stands out as the singular and well-developed male accessory gland, constituting the majority of ejaculate volume (*Leis-Filho & Fonseca-Alves, 2018; Basinger et al., 2003*).

Similar to other species, androgen hormones play a crucial role in regulating the canine prostate, ensuring its development, growth, and maintenance of secretory activity. Androgens also influence the proliferation and differentiation of luminal epithelial cells (*Sun et al., 2017*). While androgens are essential for the survival of epithelial cells and the quiescence of stromal cells, basal cell proliferation remains androgen-independent (*Hayward & Cunha, 2000*).

Castration in dogs, resulting in the absence of testosterone and subsequently dihydrotestosterone (DHT), leads to the involution of the prostate gland (*Hayward & Cunha, 2000; Leis-Filho & Fonseca-Alves, 2018*). Castration induces an immediate drop in serum testosterone levels (*Tilley & Smith Jr, 2015*).

Given the prevalence of prostatic disorders in male dogs, often associated with age, elevated DHT, and infectious agents (*Palmieri et al., 2022; Schrank & Romagnoli,*

2020), the canine prostate serves as an excellent model for human prostate structure and pathology (*Ryman-Tubb et al., 2022*).

Furthermore, canine castration is a preventive measure against androgen-dependent diseases such as benign prostatic hyperplasia (BPH) (*Ryman-Tubb et al., 2022*). This procedure proves effective, rapid, and long-lasting, causing a swift reduction in blood testosterone concentrations and decreasing glandular volume to levels comparable to healthy animals within two weeks (*Cazzuli et al., 2022*).

Therefore, the primary objective of this study is to investigate the histological features of the canine prostate gland following castration in comparison to its intact state.

Materials and Methods

Experimental animal and housing

Six apparently healthy male mongrel dogs (18–20 kg, 12–24 months) were acquired and housed under standard environmental conditions with free access to clean drinking water and a standard diet. The study took place at the Animal House, Surgery Department, Faculty of Veterinary Medicine, Suez Canal University, Ismailia, Egypt. Ethical approval was obtained from the Scientific Research Ethics Committee of the Faculty of Veterinary Medicine, Suez Canal University (**Approval number: 2022019**).

Experimental design and animal grouping

Following a week of acclimatization, animals were randomly assigned to two groups: Group I (Control - "Non-Castrated"), comprising three intact male dogs, and Group II (Bilateral Castrated Group), comprising three male dogs that underwent complete castration.

Surgical procedure

Before surgery, animals underwent a fasting period of approximately 4 hours for food and 2 hours for water. Intramuscular administration of prophylactic antibiotic cefotaxime (Cefotax, EIPICO, Tenth of Ramadan, Egypt) at a dose of 50 mg/kg and intramuscular injection of chlorpromazine hydrochloride (Neurazine, Misr Co. Pharm., Al Qalyubia, Egypt) at a dose of 1 mg/kg was performed. General anesthesia was induced and maintained by intravenous injection of thiopental sodium 2.5% solution (E.I.P.I.C.O., Egypt) according to *Clarke et al., (2014)*. Animals then underwent a closed pre-scrotal orchietomy as described by *Fossum, (2018)*.

Biochemical analysis

Blood samples were collected from the cephalic vein for serum testosterone estimation using an enzyme-linked immunosorbent assay (ELISA) with the Testosterone (Canine) ELISA Kit from Abnova (Catalog Number: KA2297).

Histological procedures

Tissue sampling and preparation

At the end of the experiment, animals were euthanized with an overdose of intravenous thiopental sodium 2.5% solution. The prostate gland was harvested, immediately fixed in an appropriate fixative, and processed for histological and immunohistochemical studies.

Histological and histochemical procedures

The fixed tissue specimens underwent dehydration, clearing, paraffin infiltration, and embedding. Paraffin blocks were sectioned at 5–7 μm thickness and processed for Hematoxylin & Eosin (H&E), Periodic Acid Schiff (PAS), Masson's Trichrome, Verhoeff's Van Gieson, and Gomori's Reticulin stains according to *Suvarna et al., (2018)*.

Immunohistochemical procedures

For Immunohistochemical examination, 4% paraformaldehyde-fixed prostatic tissue specimens were processed following routine histological procedures. Sections of 5-7 μm were cut, mounted on special slides, and subjected to immunostaining for detection of Androgen Receptor (AR). The primary AR antibody from Abclonal (catalogue number: A2053) at a dilution of 1:100 was used, and PolyDetector DAB HRP Brown detection system (catalogue number: BSB 0015, Bio SB) was employed for the reaction detection.

Image analysis and morphometric studies

Stained sections were examined and photographed using an Olympus BX 41 research microscope with a digital AMT camera at the Photomicrograph Unit of Cytology and Histology Department, Faculty of Veterinary Medicine, Suez Canal University, Ismailia, Egypt. Morphometric parameters, including epithelial height in H&E sections, percentage area of collagen fibers from Masson's trichrome sections, and mean area percent of AR immunoreactivity were analyzed using Image J software established by the National Institute of Health (Bethesda, Maryland, USA).

Statistical analysis

Data were presented as means \pm SE and statistically analyzed using SPSS (Statistical Package for Social Sciences) version 25. The Student T-test was applied, and significance was considered when P value < 0.05 , with $P \leq 0.01$ indicating high significance.

Results

Biochemical estimation of serum testosterone concentrations

According to **Fig (1)**, the bilateral castrated group showed a significant decline in serum testosterone concentrations after 20 days of bilateral castration ($P < 0.01$) compared to the control group.

Histological observations

H&E staining results

Examination of H&E-stained sections of the prostatic tissue from

the control group revealed normal lobular architecture. Prostatic lobules were formed of secretory acini of variable shapes and sizes, closely packed with scanty interstitial tissue. The glandular lining consisted of simple cuboidal or columnar epithelium with acidophilic cytoplasm and rounded to oval vesicular nuclei. Sporadic basal cells with flattened large nuclei and scanty cytoplasm were observed. The lumina of the acini contained variable amounts of acidophilic secretion (**Fig. 2A**).

Contrastingly, the prostatic specimens of the bilateral castrated group revealed alterations in the histological structure of the acini and stroma. There was an apparent reduction in the size of the acini and lumen compared to the control group. The epithelial lining altered to be low cuboidal, and the interacinar connective tissue became thick (**Fig. 2B**).

Histochemical staining results

The PAS-stained sections of the prostate gland obtained from the control group showed a PAS-positive reaction in the apical cytoplasm of the epithelial lining (**Fig. 2C**). In contrast, prostatic sections from the bilateral castrated group expressed a negative reactivity to PAS (**Fig. 2D**).

The Masson's trichrome-stained sections of the control group revealed a normal amount of collagen fibers and a thin layer of smooth muscle fibers around the acini (**Fig. 3A**). Conversely, the

bilateral castrated group demonstrated heavy deposition of collagen fibers among acini (**Fig. 3B**). The presence of a reticular fiber network supporting the prostatic acini was demonstrated in sections stained with Gomori's reticulin and was apparently similar in both groups; control group (**Fig. 3C**) and bilateral castrated group (**Fig.3D**). In addition, delicate elastic fibers were observed between the secretory units by Verhoeff's Van Gieson stain. No notable differences were detected between the experimental groups; control group (**Fig. 3E**) and bilateral castrated group (**Fig.3F**).

Androgen receptor (AR) immunostaining in prostatic tissue

In the control group, luminal epithelial cells expressed a strong positive nuclear reaction for AR (**Fig. 2E**). In contrast, the bilateral castrated group showed few acinar

cells with very weak nuclear AR immunolabeling, while all others had a negative immunoreactivity (**Fig. 2F**).

Morphometric and statistical results

Morphometric analysis of epithelial height in H&E-stained sections showed a statistically significant decrease in the bilateral castrated group compared to the control group ($P < 0.01$), (**Fig.4**).

From the prostatic tissue section stained with Masson's Trichrome, the bilateral castrated group revealed a highly significant increase in the mean area % of collagen fibers ($P < 0.01$) compared to the control (**Fig.4**).

Concerning the mean % area of AR immunolabeling, a significant reduction in the bilateral castrated group was observed compared to the control ($P < 0.01$), (**Fig.4**).

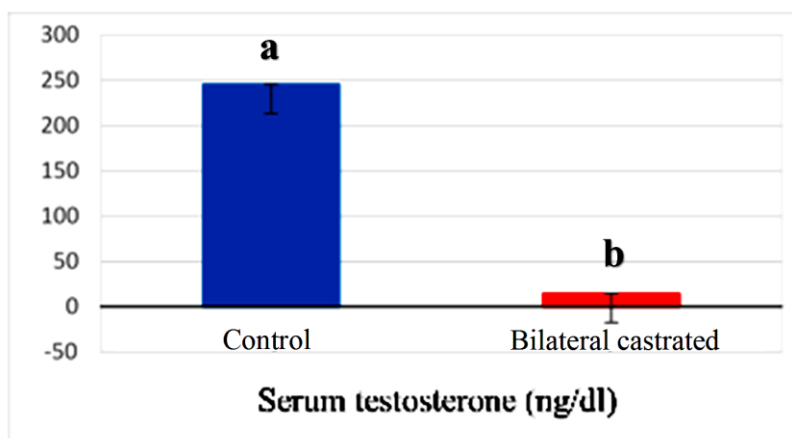


Fig.1: Serum testosterone level was measured for the Control and Bilateral castrated groups. All data were represented as mean \pm SE. Means with different superscripts are statistically significant ($P \leq 0.01$).

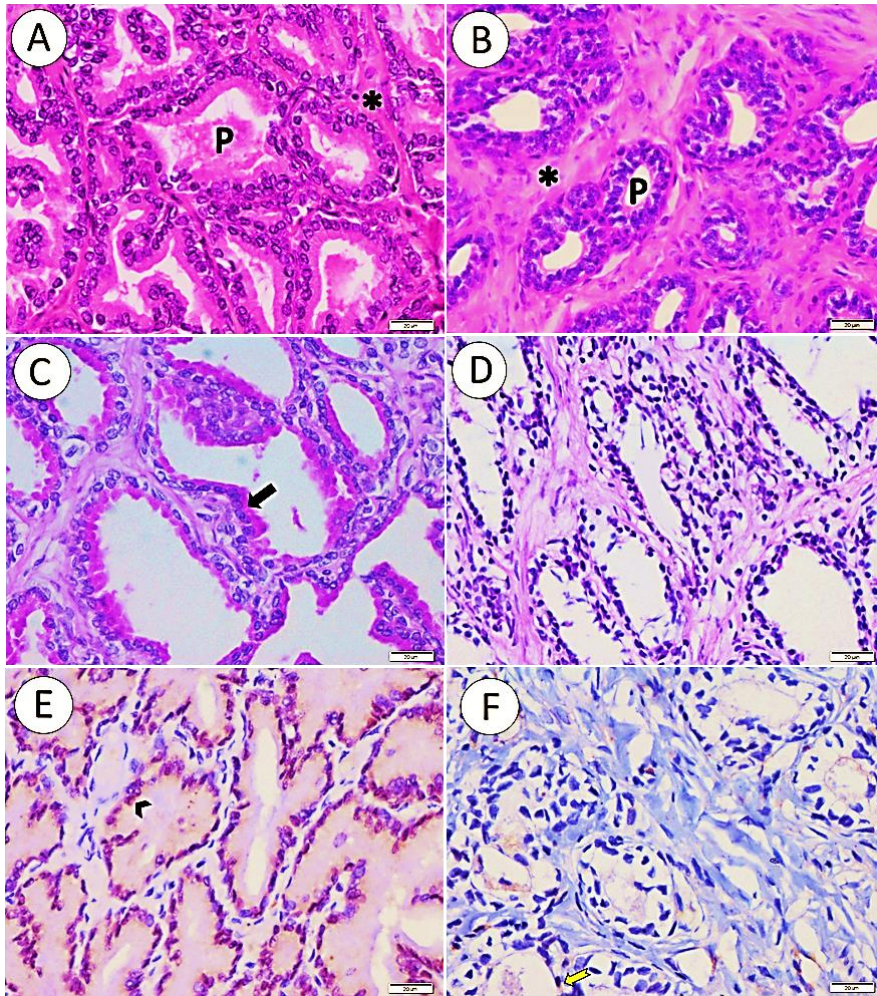


Fig.2: Photomicrographs of prostatic tissue. (A&B) H&E-stained sections showing histological features of prostatic lobules. A: Control group demonstrating prostatic acini (P) containing secretion and separated by scanty interstitial tissue (*). B: Bilateral castrated group showing collapsed acini (P) embedded in thick stromal tissue (*). (C&D) Prostatic tissue stained with PAS. C: Control group showing strong positive reactivity of lining epithelium cytoplasm (arrow). D: Bilateral castrated group demonstrating PAS negative reaction of prostatic acinar epithelial lining. (E&F) Immunohistochemical stained prostatic tissue for AR. E: Control group illustrating strong positive nuclear AR immunolabelling of secretory cells (arrowhead). F: Bilateral

castrated group showing only few cells have very weak positive nuclear AR expression (notched arrow) while others are negative.

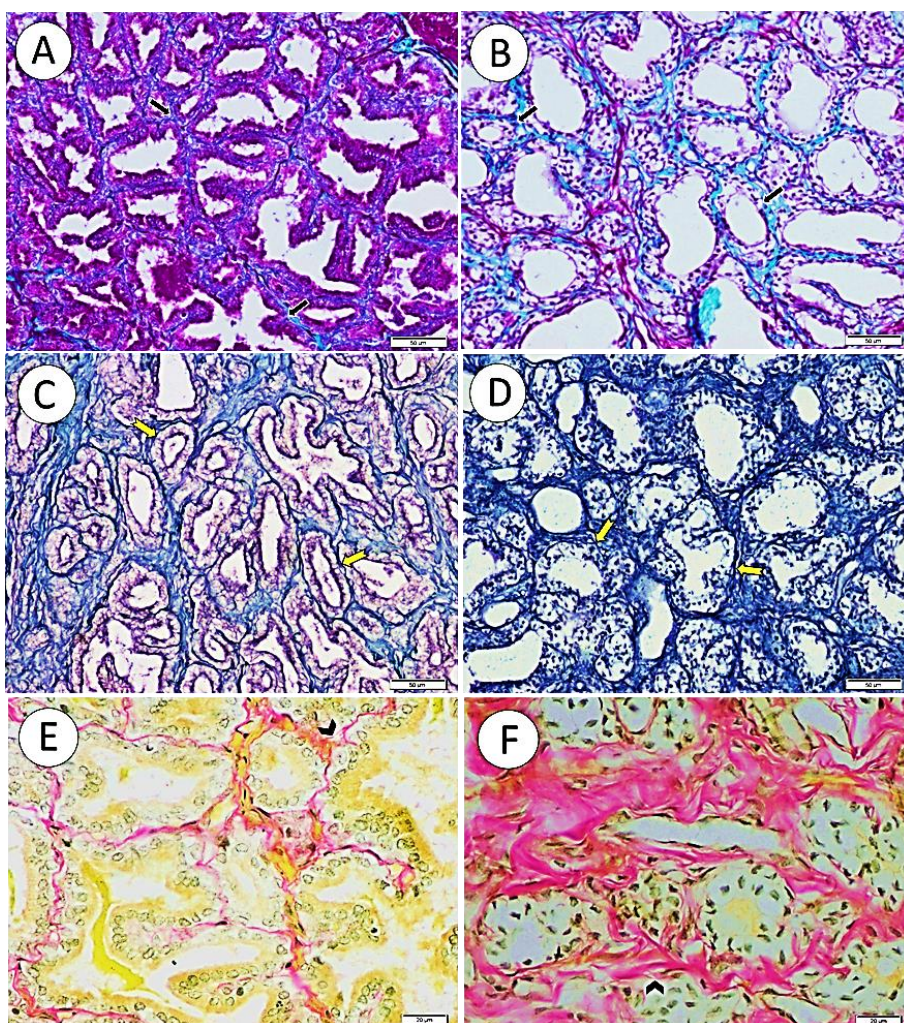


Fig.3| Photomicrographs of prostatic tissue demonstrating the interstitial tissue. (A&B) Masson's trichrome-stained sections illustrating interstitial collagen (arrows). A: Control group showing few interstitial collagen fibers. B: Bilateral castrated group revealing abundant collagen fibers deposition. (C&D) Gomori's reticulin-stained sections demonstrating the reticular fiber network (notched arrows) supporting prostatic acini. C: Control group and D: Bilateral castrated group showing normally distributed reticular fibers. (E&F) Verhoeff's Van Gieson-stained sections showing delicate elastic fibers (arrowhead) of interstitial tissue. E: Control group and F: Bilateral castrated group revealing nearby similar distribution pattern of elastic fiber.

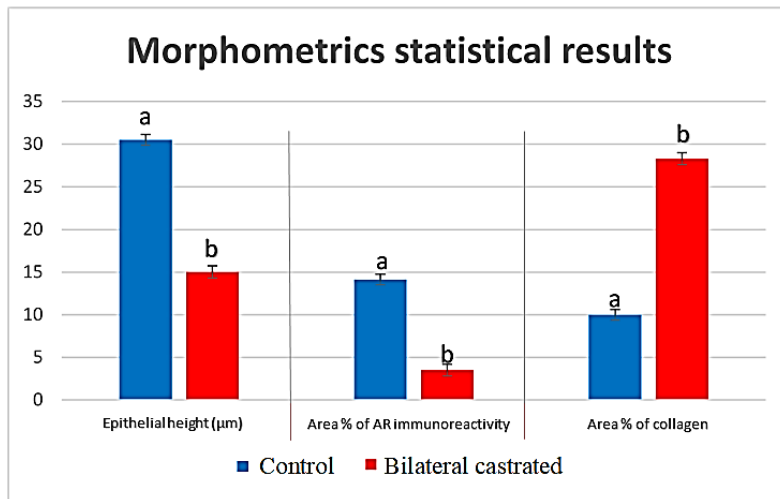


Fig.4| The epithelial heights (μm), the area % of AR immunoreactivity and the area% of collagen fibers in prostatic tissue was measured in Control and Bilateral castrated groups. All data were represented as mean \pm SE. Means with different superscripts are statistically significant ($P \leq 0.01$).

Discussion

In this study, a highly significant decline in serum testosterone levels was observed after bilateral castration, consistent with findings in rats by (*Felix-Patricio et al., 2017*) The reduction in testosterone can be attributed to the absence of testes, the primary site of testosterone production (*Salavati et al., 2018*).

The histological examination of non-castrated animals revealed a normal lobular architecture of the prostate gland, with closely packed acini lined by columnar cells, consistent with previous studies (*Al-Omari et al., 2005; Hammodi & Hamza, 2022; Lai et al., 2008; Leis-Filho &*

Fonseca-Alves, 2018). Positive reactivity to PAS in the apical cytoplasm of luminal cells indicated the presence of neutral mucopolysaccharides (*Hammodi & Hamza, 2022*).

Immunohistochemical analysis showed a strong positive AR immunoreactivity of luminal cells, supporting the importance of testosterone levels and AR expression for normal prostatic epithelium (*Dai et al., 2017*).

After bilateral castration, distinct alterations in histological architecture were observed, including a reduction in acini size, low cuboidal epithelium, and loss of cytoplasmic acidophilia. These

changes align with previous studies (*Al-Omari et al., 2005; Campos et al., 2010*) and suggest epithelial reduction and atrophy post-castration. The negative reactivity to PAS indicated a lack of secretory activity, consistent with hormonal prostatic atrophy observed in dogs following neutering (*Palmieri et al., 2019*).

Immunohistochemical analysis revealed weak AR immunoreactivity and negative cells after bilateral castration, indicative of reduced androgen sensitivity and secretory epithelial loss. Similar results were reported in rats, where castration led to a decline in AR-positive cells that increased after androgen replacement (*Felisbino et al., 2019; Shidaifat et al., 2004*).

Also, the present histochemical investigations of intact animal showed that secretory units of the prostate gland were surrounded by scanty interstitial tissue that made up of collagen fibers and a thin layer of smooth muscle fiber was seen by Masson's trichrome, a network of reticular fibers around the glandular end pieces was observed in Gomori reticulin sections, and fine elastic fibers between the secretory units by the Verhoef's as that observed by (*Marettová, 2017*).

Histochemical findings in the bilateral castrated group indicated interstitial tissue thickening, an increase in collagen fibers, and normal distribution of reticular and elastic fibers. These changes align with studies showing an influence of

androgen depletion on collagen fibers, while reticular fibers remain unaffected (*Felix-Patricio et al., 2017; Al-Omari et al., 2005*).

Morphometric analysis supported these findings, showing a significant decline in epithelial height, reduction of AR immunoreactivity, and an increase in the mean area % of interacinar collagen fibers in the bilateral castrated group compared to the control. Similar results were observed in castrated ferrets and neutered rats (*Bo et al., 2019; Felix-Patricio et al., 2017*).

Conclusions

In conclusion, this study demonstrated significant histological alterations in the prostatic tissue, both in stromal and glandular components, following bilateral castration, corresponding to the ablation of testosterone. These findings contribute to a broader understanding of the impacts of castration on the prostate gland and may have implications for therapeutic and preventive strategies in androgen-dependent conditions.

References

- Al-Omari, R., Shidaifat, F., & Dardaka, M. (2005).** Castration induced changes in dog prostate gland associated with diminished activin and activin receptor expression. *Life sciences*, 77(22), 2752-2759.
- Basinger, R., Robinette, C., & Spaulding, K. (2003).** Prostate.

Textbook of small animal surgery, 2, 1542-1557.

Bo, P., Tagliavia, C., Canova, M., De Silva, M., Bombardi, C., & Grandis, A. (2019). Comparative characterization of the prostate gland in intact, and surgically and chemically neutered ferrets. *Journal of Exotic Pet Medicine*, 31, 68-74.

Campos, S. G., Gonçalves, B. F., Scarano, W. R., Corradi, L. S., Santos, F. C., Custodio, A. M., Vilamaior, P. S., Goes, R. M., & Taboga, S. R. (2010). Tissue changes in senescent gerbil prostate after hormone deprivation leads to acquisition of androgen insensitivity. *International Journal of Experimental Pathology*, 91(5), 394-407.

Cazzuli, G., Damián, J. P., Molina, E., & Pessina, P. (2022). Post-castration prostatic involution: A morphometric and endocrine study of healthy canines and those with benign prostatic hyperplasia. *Reproduction in domestic animals*, 57(2), 157-164.

Clarke, K., Trim, C., & Hall, L. (2014). Anaesthesia of the dog. *Veterinary anaesthesia*, 405-498.

Dai, C., Heemers, H., & Sharifi, N. (2017). Androgen signaling in prostate cancer. *Cold Spring Harbor perspectives in medicine*, 7(9).

Felisbino, S. L., Sanches, B. D. A., Delella, F. K., Scarano, W. R., Dos Santos, F. C. A., Vilamaior, P. S. L., Taboga, S. R., & Justulin, L. A.

(2019). Prostate telocytes change their phenotype in response to castration or testosterone replacement. *Scientific reports*, 9(1), 3761.

Felix-Patricio, B., Miranda, A. F., Medeiros, J. L., Gallo, C., Gregório, B. M., Souza, D. B. d., Costa, W. S., & Sampaio, F. J. (2017). The prostate after castration and hormone replacement in a rat model: structural and ultrastructural analysis. *International braz j urol*, 43, 957-965.

Fossum, T. W. (2018). *Small animal surgery e-book*. Elsevier Health Sciences.

Hammodi, M. I., & Hamza, L. O. (2022). Histological and histochemical observations of the prostate gland at resting and stimulating status in adult local dog (*Canis familiaris*). *Iraqi Journal of Veterinary Sciences*, 36(3), 605-610.

Hayward, S. W., & Cunha, G. R. (2000). The prostate: development and physiology. *Radiologic Clinics of North America*, 38(1), 1-14.

König, H., & Liebich, H. (2020). *Veterinary Anatomy of Domestic mammals: Textbook and colour Atlas, 7th, update and extended edition*. Georg Thieme Verlag Stuttgart

Lai, C. L., van den Ham, R., van Leenders, G., van der Lugt, J., & Teske, E. (2008). Comparative characterization of the canine normal prostate in intact and

castrated animals. *The Prostate*, 68(5), 498-507.

Leis-Filho, A. F., & Fonseca-Alves, C. E. (2018). Anatomy, histology, and physiology of the canine prostate gland. In *Veterinary Anatomy and Physiology* (pp. 47-67). IntechOpen London, UK.

Marettová, E. (2017). Immunohistochemical localization of elastic system fibres in the canine prostate. *Folia Veterinaria*, 61(1), 5-10.

Palmieri, C., Fonseca-Alves, C. E., & Laufer-Amorim, R. (2022). A review on canine and Feline prostate pathology. *Frontiers in Veterinary Science*, 9, 881232.

Palmieri, C., Foster, R., Grieco, V., Fonseca-Alves, C., Wood, G., Culp, W., Escobar, H. M., De Marzo, A., & Laufer-Amorim, R. (2019). Histopathological terminology standards for the reporting of prostatic epithelial lesions in dogs. *Journal of comparative pathology*, 171, 30-37.

Ryman-Tubb, T., Lothion-Roy, J. H., Metzler, V. M., Harris, A. E., Robinson, B. D., Rizvanov, A. A., Jeyapalan, J. N., James, V. H., England, G., & Rutland, C. S. (2022). Comparative pathology of dog and human prostate cancer. *Veterinary medicine and science*, 8(1), 110-120.

Salavati, S., Mogheiseh, A., Nazifi, S., Tabrizi, A. S., Taheri, P., & Koohi, F. (2018). Changes in sexual hormones, serotonin, and cortisol concentrations following oral administration of melatonin in castrated and intact dogs. *Journal of Veterinary Behavior*, 27, 27-34.

Schrank, M., & Romagnoli, S. (2020). Prostatic neoplasia in the intact and castrated dog: How dangerous is castration? *Animals*, 10(1), 85.

Shidaifat, F., Daradka, M., & Al-Omari, R. (2004). Effect of androgen ablation on prostatic cell differentiation in dogs. *Endocrine research*, 30(3), 327-334.

Sun, F., Báez-Díaz, C., & Sánchez-Margallo, F. M. (2017). Canine prostate models in preclinical studies of minimally invasive interventions: Part I, canine prostate anatomy and prostate cancer models. *Translational andrology and urology*, 6(3), 538-546.

Suvarna, K. S., Layton, C., & Bancroft, J. D. (2018). *Bancroft's theory and practice of histological techniques*. Elsevier health sciences.

Tilley, L. P., & Smith Jr, F. W. (2015). *Blackwell's five-minute Veterinary consult: canine and feline*. John Wiley & Sons.

دراسات نسيجية، نسيجوكيميائية ونسيجوكيميائية مناعية لغدة البروستاتا في الكلاب مخصية الجانبيين

سامح محمد فاروق¹، أمل عرفات مختار أحمد¹، محمد عبدالله هاشم²،

صفا حسام الدين بدران^{3*}

¹قسم الخلية والأنسجة، كلية الطب البيطري، جامعة قناة السويس، الإسماعيلية، مصر

²قسم الجراحة والتخدير والأشعة، كلية الطب البيطري، جامعة قناة السويس، الإسماعيلية، مصر

³قسم الخلية والأنسجة، كلية الطب البيطري، جامعة العريش، شمال سيناء، مصر

الملخص العربي

تعتبر غدة البروستاتا واحدة من الأعضاء التي يرتبط نشاطها بالاندروجين. إضافة إلى ذلك يعد الإخصاء وسيلة شائعة لعلاج الأمراض المرتبطة بالتستوستيرون. لذلك هدفت الدراسة الحالية إلى دراسة التركيب النسيجي لغدة البروستاتا في ذكور الكلاب البالغة بعد استئصال الخصية. تم تقسيم عدد ست كلاب ذكور (18-20 كجم، 12-24 شهرًا) إلى مجموعتين: المجموعة الأولى (الضابطة) والمجموعة الثانية تم استئصال الخصيتين جراحياً. تم قياس مستويات هرمون التستوستيرون في الدم. كما تم جمع العينات النسيجية للبروستاتا في اليوم العشرين لإجراء الدراسات النسيجية والنسيجوكيميائية المناعية. أدى الإخصاء الكلي إلى انخفاض سريع في مستوى هرمون التستوستيرون في الدم وصاحب ذلك تغيرات نسيجية واضحة في غدة البروستاتا والتي يمكن تلخيصها في انخفاض كبير في القياسات المورفومترية الدالة على فقدان الوظيفة الإفرازية لغدة البروستاتا حيث أن الاستجابة لمستقبلات الاندروجين قلت بصورة ملحوظة. علاوة على ذلك، كان هناك زيادة ظاهرة في النسيج الخلالي، والتي تتميز بزيادة كبيرة في نسبة ألياف الكولاجين. تبين مما سبق أن الإخصاء الكلي يسبب تغيرات نسيجية واضحة في التركيب النسيجي للبروستاتا توازياً مع انخفاض مستوى هرمون التستوستيرون في الدم.